Regulation of cortactin/dynamin interaction by actin polymerization during the fission of clathrin-coated pits

Jianwei Zhu, Kang Zhou, Jian-Jiang Hao, Jiali Liu, Nicole Smith and Xi Zhan*

Department of Pathology, Greenebaum Cancer Center, University of Maryland School of Medicine, 15601 Crabbs Branch Way, Rockville, MD 20855, USA

*Author for correspondence (e-mail: szhan001@umaryland.edu)

Accepted 29 November 2004
Journal of Cell Science 118, 807-817 Published by The Company of Biologists 2005
doi:10.1242/jcs.01668

Summary

Separation of clathrin-coated pits from the plasma membrane, a key event during endocytosis, is thought to be driven by dynamin and the actin cytoskeleton. However, the mechanism for the actin-mediated endocytosis remains elusive. RNA interference-mediated suppression of cortactin, an F-actin binding protein that promotes Arp2/3 complex-mediated actin polymerization, effectively blocked transferrin uptake. Depletion of cortactin in brain cytosol inhibited formation of clathrin-coated vesicles by 70% as analyzed in a cell-free system. Interestingly, the interaction between cortactin and dynamin 2 in cells was dependent on actin polymerization and was attenuated upon cell exposure to cytochalasin D as analyzed by immunofluorescence and immunoprecipitation. Moreover, a cortactin mutant deficient in Arp2/3 binding colocalized less efficiently with dynamin 2 and inhibited the uptake of transferrin. The effect of actin polymerization on the interaction between cortactin and the dynamin proline-rich domain (PRD) was further evaluated under a condition for actin polymerization in vitro. Cortactin binds to the dynamin PRD with an equilibrium dissociation constant of 81 nM in the presence of the Arp2/3 complex and actin, and 617 nM in the absence of actin polymerization. Taken together, these data demonstrate that Arp2/3-mediated actin polymerization regulates the accessibility of cortactin to dynamin 2 and imply a novel mechanism by which cortactin and dynamin drive the fission of clathrin-coated pits in an actin polymerization dependent manner.

Key words: Cortactin, Dynamin, Actin polymerization, Clathrin-coated vesicles, Endocytosis

Introduction

Clathrin-mediated endocytosis, a major cellular pathway for internalization of proteins and lipids as well as recycling of synaptic vesicles, is comprised of a series of sequential events including ligand-receptor binding, coat assembly, formation of clathrin-coated vesicles (CCVs), and membrane fission to release CCVs that subsequently move into the deeper cytosol (Cousin, 2000; Deitcher, 2002; Hinshaw, 2000; Qualmann and Kessels, 2002; Sever, 2002). One of the key molecular events in the process is the recruitment of dynamin, a family of proteins with an intrinsic GTPase activity, into the neck of CCV wherein dynamin participates in the late stages of vesicle invagination and fission (Bottomley et al., 1999; Hinshaw, 2000). Dynamin contains a proline-rich domain (PRD) at the C-terminus, which is known to bind to multiple SH3-containing proteins, including Grb2 (Gout et al., 1993), intersectin (Roos and Kelly, 1998), endophilin (Ringstad et al., 1997), syndaptin I (Qualmann et al., 1999), amphiphysin I (David et al., 1996), amphiphysin II (Ramjaun et al., 1997), profilin (Witke et al., 1998) and mammalian Abp1 (Kessels et al., 2001). Although it has been reported that peptides encoding the SH3 domain from most of these proteins can inhibit endocytosis by disrupting either the formation of constricted CCVs or late events for the fission of membrane (Simpson et al., 1999), the specific mechanism by which these proteins regulate endocytosis remains elusive.

There is growing evidence that dynamin may act in concert with the actin cytoskeleton as a mechano-enzyme during endocytosis (Engqvist-Goldstein et al., 2003; Qualmann and Kessels, 2002). A recent study has demonstrated that invagination of CCVs occurs immediately after a brief burst of dynamin recruitment into CCVs followed by transient actin assembly, indicating that dynamin may trigger actin polymerization (Merrifield et al., 2002). Although the detailed mechanism by which dynamin links to or triggers actin assembly is unclear, several actin cytoskeleton-associated proteins have been found to interact with dynamin in cells (Orth and McNiven, 2003). One of the proteins that plays a role in linking dynamin to actin assembly is cortactin (McNiven et al., 2000), which is an SH3-containing protein that binds to Arp2/3 complex and also promotes actin assembly (Uruno et al., 2001; Weaver et al., 2001). The role of cortactin in endocytosis was first recognized in an immunofluorescent analysis showing that cortactin associates with endosomes along with the Arp2/3 complex (Kaksonen et al., 2000). An electron microscopy study further indicated that cortactin is distributed over the surface or base of clathrin lattices, as well as actin filaments associated with the pits (Cao et al., 2003).

Studies based on microinjection of anti-cortactin antibody or transfection of a plasmid encoding the cortactin SH3 domain further support the role of cortactin in receptor-mediated endocytosis (Cao et al., 2003). However, the precise role of cortactin in the invagination and fission of clathrin-coated pits mediated by dynamin is not known.

Our previous study and the work of others have demonstrated that cortactin promotes actin polymerization mediated by the Arp2/3 complex (Uruno et al., 2001; Weaver et al., 2001). In contrast to WASP family members, which activate the Arp2/3 complex in a G-actin binding dependent manner (Hufner et al., 2001), cortactin contains an Arp2/3 complex binding motif followed by an F-actin binding domain that is comprised of a characteristic six-and-a-half 37-amino acid repeats. This structural feature renders a unique property to cortactin such that its affinity for the Arp2/3 complex is regulated by actin assembly (Uruno et al., 2003). Under physiological conditions for actin assembly, cortactin binds to the Arp2/3 complex as well as F-actin with an affinity approximately 40-fold higher than that in the absence of actin polymerization. Hence, cortactin, the Arp2/3 complex and its associated nascent actin filaments probably form a tight complex only in the areas where actin polymerization is actively taking place. However, the significance of this unique property of cortactin in endocytosis has not yet been explored. In particular, it is unclear whether the apparent association of cortactin with dynamin is a cause or a consequence of endocytosis-initiated actin assembly. The mechanism by which cortactin-mediated actin assembly induces invagination of vesicles, which is essentially an inward membrane, is also unknown.

In the present study, we show that cortactin participates in CCV formation in a manner depending on actin polymerization. In addition, we examine the interaction between dynamin 2 and cortactin both in vitro and in vitro under physiological conditions for actin assembly. We found that the process of actin polymerization mediated by Arp2/3 complex is prerequisite for the interaction of cortactin with dynamin. Thus, the accessibility of the cortactin SH3 domain to dynamin is optimized during the course of actin polymerization. Instead of triggering actin assembly, we suggest that cortactin engaging in actin assembly has a motor function to drive the fission of clathrin-coated pits through dynamin binding and removes dynamin-associated vesicles from the protrusive membrane.

Materials and Methods

Antibodies and other reagents

Anti-cortactin polyclonal antibody was prepared as described (Liu et al., 1999). Other antibodies include: anti-cortactin and anti-GST (Upstate); chicken anti-human transferrin antibody (ICN Biomedicals); anti-biotin (Pierce); anti-GFP, anti-rabbit and anti-mouse IgG (Molecular Probes); monoclonal dynamin antibodies (Upstate and BD); polyclonal dynamin 2 antibody (MC63) (a gift from M. A. McNiven, Mayo Clinic). Other reagents are: Oregon Green 488-labeled transferrin (Molecular Probes), N-hydroxysuccinimide (NHS)-SS-biotin and goat anti-biotin (Pierce), rat brain (PelFreeze), rabbit skeletal muscle actin (Cytoskeleton), Lipofectamine DNA transfection reagent (Life Technologies), protein A Sepharose, glutathione Sepharose 4B and ECL western blot detection reagents (Amersham Biosciences). Reagents from Sigma include: diferric-transferrin, biotin-transferrin, sodium 2-mercaptoethanesulfonate (MesNa), iodoacetic acid (IAA), dimethyl pimelimidate dihydrochloride (DMP), ATP, GTP, creatine phosphokinase, sodium creatine phosphate dibasic tetrahydrate and TRITC-Phalloidin.

DNA constructs and recombinant proteins

His-cortactin, GST-VCA and Arp2/3 complex were purified as described previously (Uruno et al., 2001). Plasmids of cortactin-GFP and cortΔ(1-23)-GFP have been described previously (Li et al., 2004). Dyn-GFP plasmid was a gift from M. A. McNiven.

To prepare GST-Dyn-PRD, a DNA fragment encoding the proline-rich domain of rat dynamin 2 was generated by PCR using Dyn-GFP as a template and then inserted into pGEX-4T2 plasmid at *Eco*RI-*Xho*I sites. The resulting plasmid was transformed into bacterial BL21 (DE3) pLysS strain for protein expression. To purify GST-Dyn-PRD protein, bacteria were grown at 37°C to an OD_{600} of 0.6, and gene expression was induced by adding isopropyl-β-D-thiogalactopyranoside (IPTG) to a final concentration of 0.5 mM. The induced bacteria were grown for additional 3 hours and harvested by centrifugation at 6000 ***g*** for 10 minutes. The bacterial pellet was resuspended in 1/10 volume of starting culture of PBS containing 2.5 mM DTT and 20 mg/ml PMSF. The suspension was homogenized with an ultrasonic processor (Heat Systems, Ultrasonics) at power setting of 4 with 20 pulses per cycle up to ten cycles. Lysates were clarified by centrifugation at 15,000 ***g*** for 20 minutes at 4°C. The supernatant was filtered through a 0.22 mm sterilizing filter unit (Fisher Scientific) and loaded onto a mini glutathione Sepharose 4B column (Amersham Pharmacia Biotech), which was washed extensively with lysis buffer. GST-tagged protein was eluted in the lysis buffer containing 10 mM glutathione. The eluted fraction was subjected to dialysis against PBS, aliquoted and kept in –80°C.

Cell culture and immunofluorescence assay

HeLa and MDA-MB-231 cells were grown in Dulbecco's modified Eagle's medium (DMEM) supplemented with 10% fetal calf serum (FCS). 3T3-L1 and NIH3T3 cells were grown in DMEM with 10% calf serum. For immunofluorescence assay, cells were grown on coverslips in a six-well plate and treated with fluorescent antibodies as described (Li et al., 2001). Briefly, cells were fixed with 4% formaldehyde, permeabilized with 0.2% Triton X-100, and incubated with primary and secondary antibodies, in 0.1% BSA-PBS. Stained cells were inspected either using an inverted Nikon ECLIPSE TE2000-U microscope equipped with a digital camera controlled by Nikon ACT-1 software, or using a Radiance laser scanning 2100 confocal system. All digital images were captured at the same settings to allow direct quantitative comparison of staining patterns. Final images were processed using Adobe Photoshop software. Fluorescent intensity of green transferrin was measured by Nikon ACT-1 software and further analyzed by Scion Image. Confocal colocalization assay between two fluorescent stainings was performed using Optimas 5.2 image-analysis software as described previously (Uruno et al., 2001).

RNA interference, cytochalasin D treatment and immunoprecipitation

Cortactin siRNAs were prepared by an in vitro transcription procedure using T7 RNA polymerase according to the manufacturer's protocol of Silencer siRNA construction Kit (Ambion). The target sequences are: H1, AAGCTGAGGGAGAATGTCTTT; H2, AAGTTTGGTG-TCCAGATGGAC; H3, AAGTATGGGGTGCAGAAGGAT.

The day before transfection, HeLa cells were seeded on six-well plates at a density of 0.8×10^5. Transfection of siRNA (50 μM) was performed according to the manufacturer's protocol for Lipofectamine transfection (Life Technologies). 24 hours after

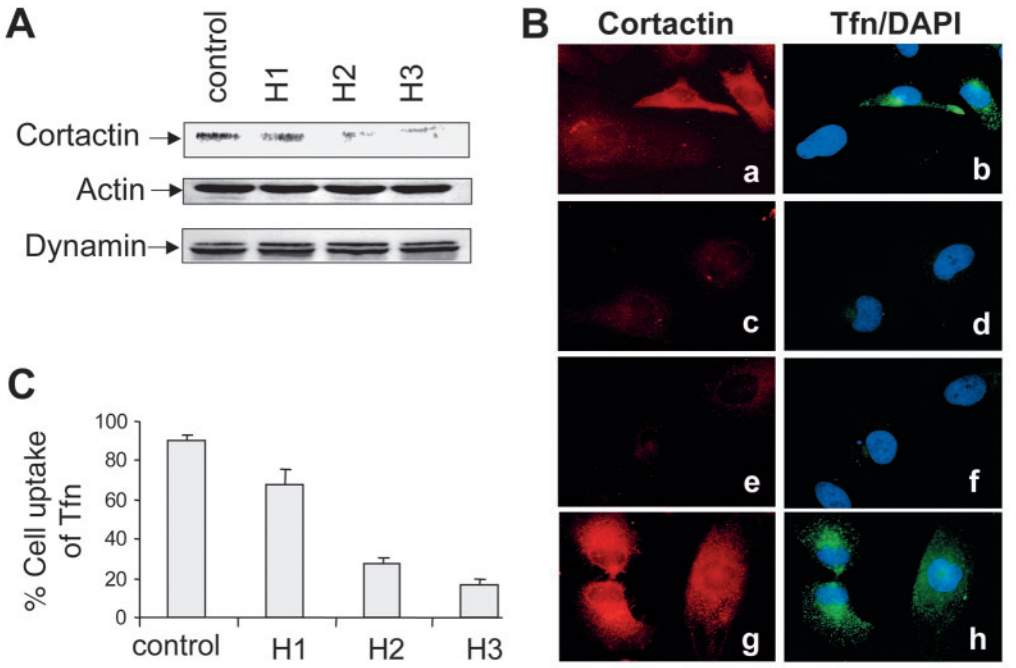

Fig. 1. Knockdown of cortactin expression attenuates transferrin uptake. (A) Cells grown in a six-well plate were transfected with cortactin siRNAs H1, H2, H3 and GFP siRNA as described in Materials and Methods. After 24 hours of transfection, cortactin expression in the treated cells was examined by immunoblot analysis. The same samples were also analyzed for actin and dynamin expression as negative controls. (B) Cells transfected with cortactin siRNA H1 (a and b), H2 (c and d), H3 (e and f) and GFP siRNA (g and h) were incubated with Oregon Green-labeled transferrin at 37°C for 30 minutes, fixed and stained with cortactin antibody (a,c,e and g) and DAPI (b,d,f and h). Internalized transferrin was seen as green dots in the cytoplasm. Magnification ×600. (C) Percentage uptake of transferrin was quantified based on the fluorescence intensity of internalized transferrin in treated cells. The data shown are mean ± s.e.m. (n>400).

transfection, cells were subjected to transferrin uptake analysis or immunoblot to confirm the silencing of cortactin expression.

To analyze the role of actin polymerization in endocytosis, NIH3T3 cells (1×10^5) grown in serum-free medium were treated with 10 μM cytochalasin D in DMSO. Control cells were treated with DMSO only. After 1 hour of treatment, cells were incubated with biotin-transferrin (20 μg/ml) for 10 minutes. In one parallel experiment, the cytochalasin D-treated cells were washed once with serum-free medium and incubated in serum-free medium for additional 1 hour before adding transferrin. The treated cells were fixed in 4% paraformaldehyde and permeabilized with PBS containing 0.2% Triton X-100. The permeabilized cells were subsequently stained with dynamin 2 and cortactin antibodies.

For immunoprecipitation analysis, NIH3T3 cells were grown in 100 mm dishes to 90% confluence, serum-starved overnight and treated with 10 μM cytochalasin D or DMSO for 0, 30, 60 or 90 minutes. The treated cells were then incubated for an additional 10 minutes in the presence of transferrin (20 μg/ml), rinsed with ice-cold PBS and scraped into 1 ml lysis buffer (5 mM HEPES, pH 7.4, 25 mM NaCl, 10% glycerol, 0.5% Nonidet P-40, 1 mM sodium vanadate, 1 mM ammonium molybdate, 0.2 mM EDTA, 0.5 mM ATP and protease inhibitor cocktail). The lysates were immunoprecipitated with anti-dynamin 2 antibody and the pellets were further immunoblotted with anti-cortactin antibody. The membrane was stripped and reblotted with dynamin antibody for quantitative normalization.

To analyze transferrin uptake, NIH3T3 cells were treated with cytochalasin D as above. The treated cells were rinsed with DMEM twice and incubated with biotin-labelled transferrin (20 μg/ml) in serum-free medium for 10 minutes at 37°C. The cells were then placed on ice, washed with ice-cold PBS twice and then subsequently incubated on ice for 10 minutes in 25 mM MES, pH 5.0, containing 150 mM NaCl and 50 μM deferoxamine mesylate and 10 minutes in

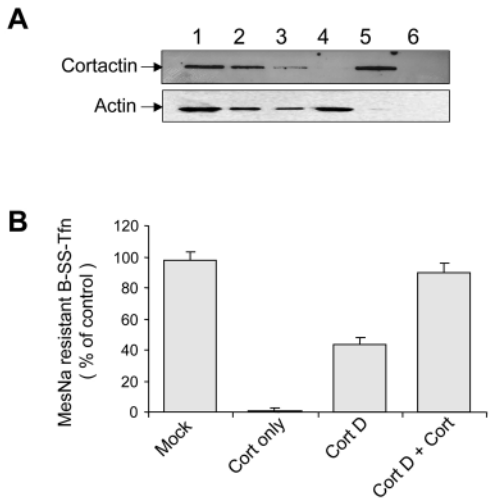

Fig. 2. Cortactin is required for the formation of clathrin-coated vesicles. (A) Rat brain extracts were depleted with beads conjugated with cortactin antibody as described in Materials and Methods. Depletion of cortactin was verified by cortactin immunoblot analysis. Non-treated brain extracts at different amounts were also analyzed (lane 1, 12 μl; lane 2, 6 μl; lane 3, 3 μl). Lane 4, 12 μl of cortactin depleted extracts; lane 5, cortactin antibody conjugated beads that had been used to absorb brain extracts; lane 6, unused cortactin antibody beads. (B) 3T3-L1 cells were permeabilized by freezing and thawing. The permeabilized cells were incubated with B-SS-Tfn at 4°C for 20 minutes and then mixed with mock-depleted brain extracts (Mock), recombinant cortactin protein in the same buffer as extracts plus 1% BSA (Cort only), cortactin-depleted extracts (Cort D), or cortactin-depleted extracts supplemented with recombinant wild-type cortactin protein (Cort D + Cort), respectively. The mixtures were incubated at 37°C for 20 minutes. The cell pellets were treated with MesNa followed by quenching with iodoacetic acid and further analyzed for the presence of the remaining Biotin-SS-Tfn in the lysates, which represents MesNa resistance and transferrin internalized into CCVs. Data shown are the mean±s.d. of three experiments.

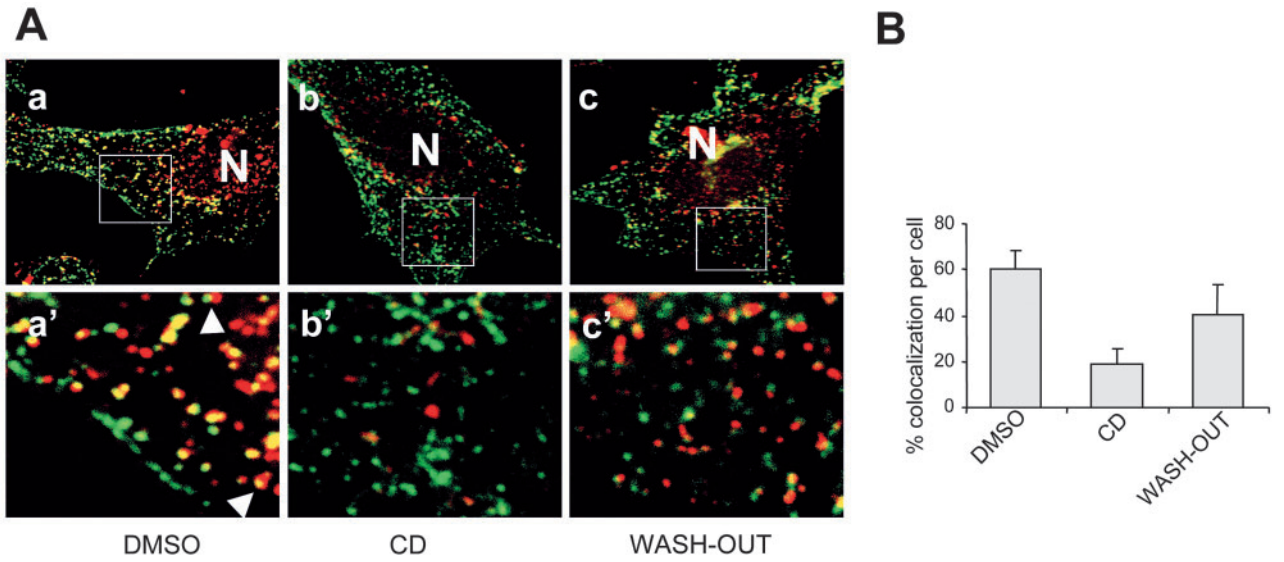

Fig. 3. Cytochalasin D disrupts the association of cortactin with dynamin 2 at endocytic sites. (A) NIH3T3 cells were treated with DMSO or 10 μM cytochalasin D in serum-free medium. After 1 hour of treatment, cells were treated with 20 μg/ml biotin transferrin and incubated for 10 minutes. In a parallel experiment, cytochalasin D was removed washed once with serum-free medium and the cells were incubated for additional 1 hour and followed by adding biotin-labeled transferrin. The treated cells were fixed, permeabilized and stained for dynamin 2 (green) and cortactin (red). The boxed regions shown in panels a, b and c were magnified and are presented in panels a′, b′ and c′, respectively. N, nucleus. Arrows in a′ indicate typical colocalization of dynamin and cortactin. Magnification ×1000. (B) Colocalization of endogenous cortactin and dynamin 2 in NIH3T3 cells was quantified using Optimas 5.2 image analysis software. The data shown are the mean±s.e.m. (n=20).

PBS. Cells were lysed with SDS sample buffer and the lysates were fractionated by SDS-PAGE followed by immunoblotting with anti-biotin antibody to detect transferrin uptake.

Capture-ELISA assay

Cells (2×10^5) stably expressing wild-type, N-terminal (1-23) truncated, and SH3 domain deleted cortactin tagged by GFP were seeded on a 12-well plate, grown in a serum-free medium containing 1% BSA and 20 mM HEPES, pH 7.4, at 37°C for 30 minutes and incubated with 10 μg/ml biotin-human transferrin (bio-Tfn) for 40 minutes on ice to allow sufficient binding. Endocytosis was initiated by re-incubating at 37°C for the times as indicated and terminated by placing on ice. The cell cultures were then treated with avidin (Sigma, St Louis, MO) and subsequently with biocytin (Sigma) to remove extracellular bio-Tfn. Cells in each well were lysed in 0.3 ml blocking buffer (1% BSA, 1% Triton X-100, 10 mM Tris-HCl, pH 7.5, 0.1% SDS, 1 mM EDTA, 50 mM sodium chloride). To measure internalized bio-Tfn, cell lysate was loaded into a 96-well ELISA plate coated with an anti-transferrin antibody (0.2 μg per well; ICN, Costa Mesa, CA) and incubated at 4°C overnight. On the next day, 100 μl streptavidin-horseradish peroxidase (HRP) conjugate (1:50,000; Roche, Nutley, NJ) was added and incubated at room temperature. After 1 hour, 100 μl tetramethylbenzidine (Roche) were applied to each well and incubated for 5 minutes. The enzymatic reaction was stopped by incubation in 1 M sulphuric acid. Light absorption at 450 nm was determined with a microplate reader to quantify the reaction product. Each assay point was performed in duplicate.

In vitro analysis of the interaction between cortactin and dynamin PRD

To analyze the affinity of GST-Dyn-PRD for cortactin, 30 nM purified GST-Dyn-PRD was mixed with immobilized His-cortactin at concentrations from 0 to 200 nM G-actin and 200 nM Arp2/3 complex in actin polymerization buffer (50 mM KCl, 2 mM $MgCl_2$, 10 mM imidazole, pH 7.5, 0.1 mM $CaCl_2$, 1 mM EGTA, 0.5 mM DTT and 0.25 mM ATP). The reaction was incubated at room temperature for 30 minutes. As a control, the reaction was also performed in the same buffer without G-actin or Arp2/3 complex. After incubation, samples were centrifuged at 800 ***g*** for 10 seconds and the supernatants were then fractionated by 12% SDS-PAGE and immunoblotted for the presence of remaining GST-Dyn-PRD with anti-GST antibody. The densities of GST-Dyn-PRD bands on the blot were scanned and quantified by Kodak Image Station 2002K and normalized to the percentage of depletion. The resulting data were used to fit a rectangular hyperbola using Sigma Plots 8.0, yielding apparent K_d values. To analyze the effect of preformed actin filaments on cortactin dynamin interaction, cortactin was incubated with G-actin and Arp2/3 complex for 20 minutes at room temperature, and GST-Dyn-PRD was then added to the reaction and incubated for additional 20 minutes. Far-western assay to confirm the direct interaction between cortactin and dynamin PRD was carried out as described (McNiven et al., 2000).

Cell-free assay for CCV formation

Rat brain cytosol was prepared as previously described (Simpson et al., 1999). Ten rat brains were diced into small pieces with a surgical blade, and homogenized using a Dounce homogenizer by 10 passes with A and B pestles, respectively, in two volumes of KSHM buffer (100 mM potassium acetate, 85 mM sucrose, 1 mM magnesium acetate and 20 mM HEPES-NaOH, pH7.4). The homogenate was then centrifuged at 10,000 ***g*** for 15 minutes, and the resulting supernatant was centrifuged further at 100,000 ***g*** for 1 hour in a Ti45 rotor. Aliquots of the resulting cytosol (supernatants) were snap-frozen in liquid nitrogen and stored at –80°C. Diferric transferrin (Sigma) was biotinylated using NHS-SS-Biotin as described (Schmid and Smythe, 1991).

To prepare cortactin-depleted cytosol, 3 mg polyclonal cortactin antibody was crosslinked to 1 ml protein A Sepharose using dimethyl pimelimidate (DMP). Isolated rat brain cytosol (3 mg) was incubated

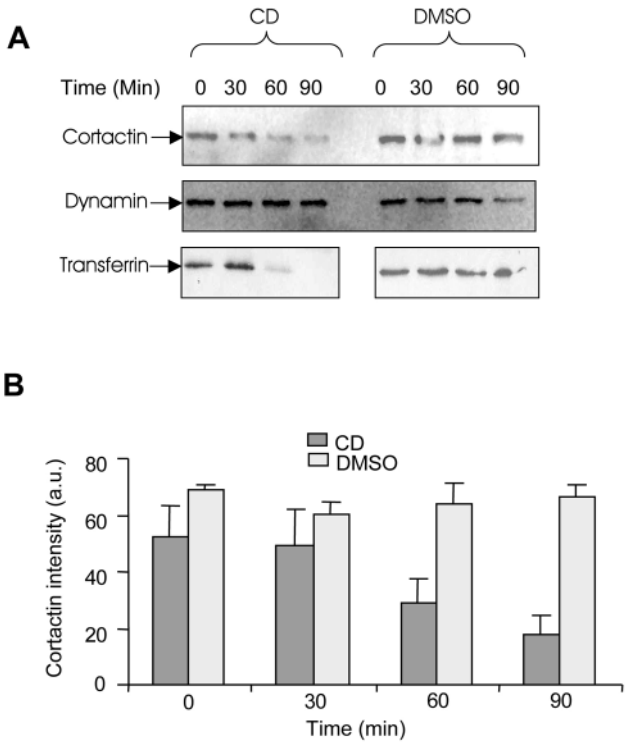

Fig. 4. Quantitative analysis of the effect of cytochalasin D on the interaction between cortactin and dynamin 2. (A) NIH3T3 cells were treated with 10 μM cytochalasin D or DMSO for 0, 30, 60 or 90 minutes, followed by transferrin treatment for addition 10 minutes. The treated cells were lysed and immunoprecipitated with dynamin antibody. The immune complex was subjected to SDS-PAGE and immunoblot assay using cortactin antibody. To measure dynamin, filters were stripped and reblotted with dynamin 2 antibody. In a parallel experiment, internalization of biotin-labeled transferrin was performed in cytochalasin D-treated cells. The internalized transferrin was detected by immunoblot analysis with biotin antibody. (B) Quantification of the interaction between cortactin and dynamin was performed based on two independent experiments and the mean±s.d. is shown.

with 0.5 ml of the cortactin affinity beads for 2 hours at 4°C and the mixture was spun briefly at 800 ***g*** for 1 minute, and the resulting cytosol was incubated with 0.5 ml of the cortactin affinity beads. The depletion efficiency was confirmed by immunoblot analysis of the cytosol. Mock-treated cytosol was prepared by passing the cytosol over goat anti-rabbit IgG-conjugated beads. To analyze the effect of cortactin only on CCV formation, 1% BSA in KSHM buffer was used as a substitute for brain cytosol. In the rescue experiments, recombinant cortactin (20 μM) was added into the cortactin-depleted cytosol.

The cell-free internalization assay with perforated 3T3-L1 cells was performed according to the methods previously described (Carter et al., 1993). 3T3-L1 cells were first washed in KSHM buffer and subjected to permeabilization by submerging in liquid nitrogen and rapidly thawing at 37°C. The cells were then scraped from culture dishes, washed for 15 minutes by rocking at 4°C in 15 ml KSHM buffer, and centrifuged at 800 ***g*** for 3 minutes. Under these conditions, >90% cells were permeabilized as assessed using Trypan Blue. The permeabilized cells (~10^7) were then incubated with 8 μg/ml biotin-SS-Transferrin (B-SS-Tfn) in KSHM buffer containing 0.8% BSA for 20 minutes at 4°C. The cell suspension (10 μl) was then mixed with ~300 μg brain cytosol (or BSA equivalent) and an ATP generating system (1 mM ATP, 8 mM creatine phosphate and 40 μg/ml creatine phosphokinase) in a final volume of 40 μl. The tubes were gently mixed and the Biotin-SS-transferrin internalization was initiated by incubation at 37°C for 20 minutes and stopped by returning to ice. After incubation, the reaction was washed with 500 μl ice-cold KSHM buffer and spun at 10,000 ***g***. After careful aspiration of the supernatants, the remaining cell pellet was then subjected to MesNa resistance assay as described (Carter et al., 1993). Briefly, the cell pellets were sequentially added with 10 mM MesNa solution (50 mM Tris, pH 8.6, 100 mM NaCl, 1 mM EDTA and 0.2% BSA) and 50 mM MesNa with a 30 minute interval and agitated at 4°C. The MesNa was quenched by addition of 500 mM iodoacetic acid for 10 minutes and the pellets were solubilized with 100 μl blocking buffer (10 mM Tris, pH 7.4, 1% Triton X-100, 0.1% SDS, 0.2% BSA, 50 mM NaCl, 1 mM EDTA). 100 μl of the cell lysate was plated on transferrin antibody-coated microtitre plates for ELISA assay to quantify internalized B-SS-Tfn with streptavidin-HRP.

Results

Cortactin is required for the receptor-mediated endocytosis and the formation of clathrin-coated vesicles

To investigate the role of cortactin in endocytosis, we studied human HeLa cells treated with cortactin small interfering RNA (siRNA) targeting different sites of cortactin mRNA and examined the effect of the cortactin siRNAs on the uptake of transferrin. Introduction of siRNA H1 modestly inhibited cortactin expression and treatment with siRNA H2 and H3 reduced cortactin expression to a trace level as demonstrated by immunoblot analysis (Fig. 1A). The siRNA-treated cells were incubated with fluorescently labeled transferrin for 30 minutes, fixed and stained with cortactin antibody (red) and DAPI (blue). The stained cells were examined for the presence of internalized transferrin (green) in the cytoplasm by fluorescence microscopy. The degree of transferrin uptake was apparently correlated with the level of cortactin expression (Fig. 1B). The cells treated with siRNA H1 with modest cortactin expression displayed only slight reduction in transferrin uptake, whereas the cells in which cortactin was nearly completely silenced showed a slow-down in transferrin uptake. A quantitative analysis based on the intensity of internalized transferrin in the cell estimated that siRNA H2 and H3 inhibited transferrin uptake by nearly 70% and siRNA H1 inhibited uptake by only 15% (Fig. 1C).

To investigate whether cortactin is implicated at an early stage of endocytosis, we utilized a functional assay based on a cell-free system that analyzes initial events immediately after membrane invagination (Carter et al., 1993; Schmid and Smythe, 1991). In this assay, transferrin labeled with biotin through a cleavable disulphide bond (B-SS-Tfn) was applied to perforated 3T3 L1 cells (Simpson et al., 1999). Under these conditions, sequestration of transferrin into deeply invaginated coated pits and internalization of coated vesicles can be reconstituted by incubation with exogenous cytosol and ATP (Carter et al., 1993; Hill et al., 2001; Schmid and Smythe, 1991; Smythe et al., 1992). As B-SS-Tfn sequestered into coated pits is resistant to MesNa, which cleaves free B-SS-Tfn, the degree of CCV formation can be quantified based on MesNa resistance. As a result, we prepared rat brain cytosol extract treated with a cortactin antibody, which depleted cortactin proteins completely but had no effect on actin in the

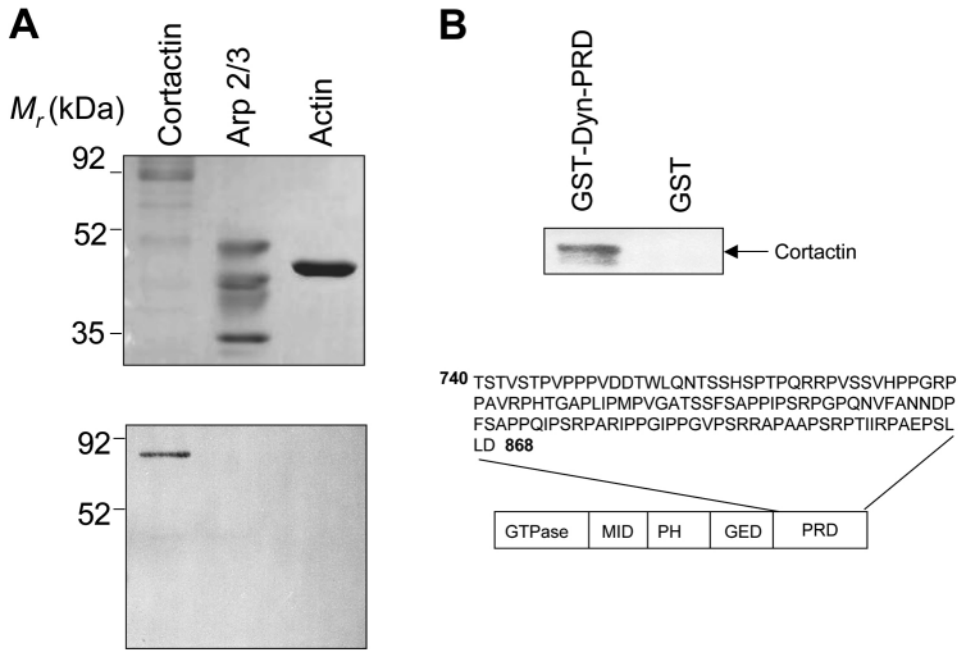

Fig. 5. Dynamin proline-rich domain binds directly to cortactin. (A) Far-western blot analysis of interaction between cortactin and dynamin PRD. Recombinant His-cortactin, Arp2/3 complex and actin protein were subjected to SDS-PAGE followed by Coomassie Blue staining (upper panel) or transferred to a cellulose membrane and then incubated with a fusion protein containing dynamin PRD (GST-Dyn-PRD). Binding of GST-Dyn-PRD to cortactin was detected by anti-GST antibody (lower panel). (B) GST-Dyn-PRD or GST were immobilized on glutathione beads and incubated with cytosolic extracts of NIH3T3 cells at 4°C for 2 hours. Cortactin binding to beads was detected by immunoblot. The amino acid sequence of PRD in GST-Dyn-PRD, corresponding to rat dynamin 2 C-terminus, is presented in the lower panel.

extract (Fig. 2A, lane 4). The cortactin-depleted extract was incubated with 3T3 L1 cells perforated by freezing and thawing. The extract without cortactin induced CCV formation poorly with an efficiency approximately 60% less than that of the mock-treated extract (Fig. 2B). Furthermore, adding a recombinant wild-type cortactin to the depleted extract resulted in a 93% restoration of the CCV formation. However, incubation of perforated cells with recombinant cortactin in a buffer containing 1% BSA was unable to induce CCV formation (Fig. 2B, lane 2), indicating that other cellular proteins are required. Taken together, these data demonstrated that cortactin is committed to effective CCV formation, an early stage of the receptor-mediated endocytosis.

Association of cortactin with dynamin requires actin polymerization

Cortactin is known to promote Arp2/3 complex-mediated actin polymerization (Uruno et al., 2001; Weaver et al., 2001). To investigate the specific role that cortactin plays in endocytosis, we examined the effect of cytochalasin D, a chemical that inhibits actin polymerization, on the distribution of endogenous cortactin and dynamin 2 in NIH3T3 cells by immunocytochemistry. In the control cells without cytochalasin D treatment, both endogenous cortactin and dynamin staining was observed as numerous tiny puncta in the cytoplasm (Fig. 3A). Around 60% of the dynamin 2 (green) staining overlapped with the cortactin puncta (red) as shown by yellow coloration (Fig. 3Aa and 3B). In many overlapping stained areas, dynamin 2 appeared to be concentrated in the area at polarized ends of cortactin puncta. This distribution pattern was similar to that described previously (Orth et al., 2002). As cortactin puncta are enriched with F-actin (Li et al., 2004; Liu et al., 1999), this result implies that only partial F-actin-associated cortactin proteins interact with dynamin 2 or its associated vesicles. Upon cytochalasin D treatment for 1 hour, the number of cortactin puncta was significantly reduced (Fig. 3A b,b′). As cytochalasin D had no effect on cortactin expression (data not shown), the formation of cortactin puncta is therefore a process that is dependent upon actin assembly. In contrast, no apparent changes in dynamin staining were observed in cytochalasin D-treated cells, suggesting that association of dynamin 2 with vesicles is not dependent on actin assembly. A quantitative analysis further indicates that the association of cortactin with dynamin 2 was decreased to less than 19.3% in the cytochalasin D-treated cells when compared with that in untreated cells (Fig. 3A b,b′). This result suggests that actin assembly is at least partially necessary for cortactin to colocalize with dynamin 2 or with vesicles. To confirm whether actin assembly is sufficient to recruit cortactin to dynamin 2, cytochalasin D was removed and the treated culture was incubated for additional 1 hour to allow initiation of actin assembly. Under these conditions, association of cortactin with dynamin 2 was largely restored (Fig. 3A c,c′). In these cytochalasin D-depleted cells, the size of areas staining with cortactin appeared to be small, reflecting newly assembled actin filaments, and the polarized overlapping between cortactin and dynamin 2 is also more apparent compared to control cells (compare Fig. 3C and 3A).

We also examined the interaction between cortactin and dynamin 2 by immunoprecipitation during the course of cytochalasin D treatment. Cortactin was readily immunoprecipitated with dynamin 2 antibody (Fig. 4A). However, cytochalasin D treatment reduced the interaction between dynamin 2 and cortactin by nearly 45% at 60 minutes and 60% after 90 minutes as compared to control cells that were treated with DMSO, the solvent used for cytochalasin D (Fig. 4B). In addition, we also analyzed endocytosis of biotin-transferrin, which was apparently inhibited within 60 minutes after cytochalasin D treatment, indicating that the interaction between cortactin and dynamin 2 is functionally correlated with endocytosis in an actin assembly dependent manner.

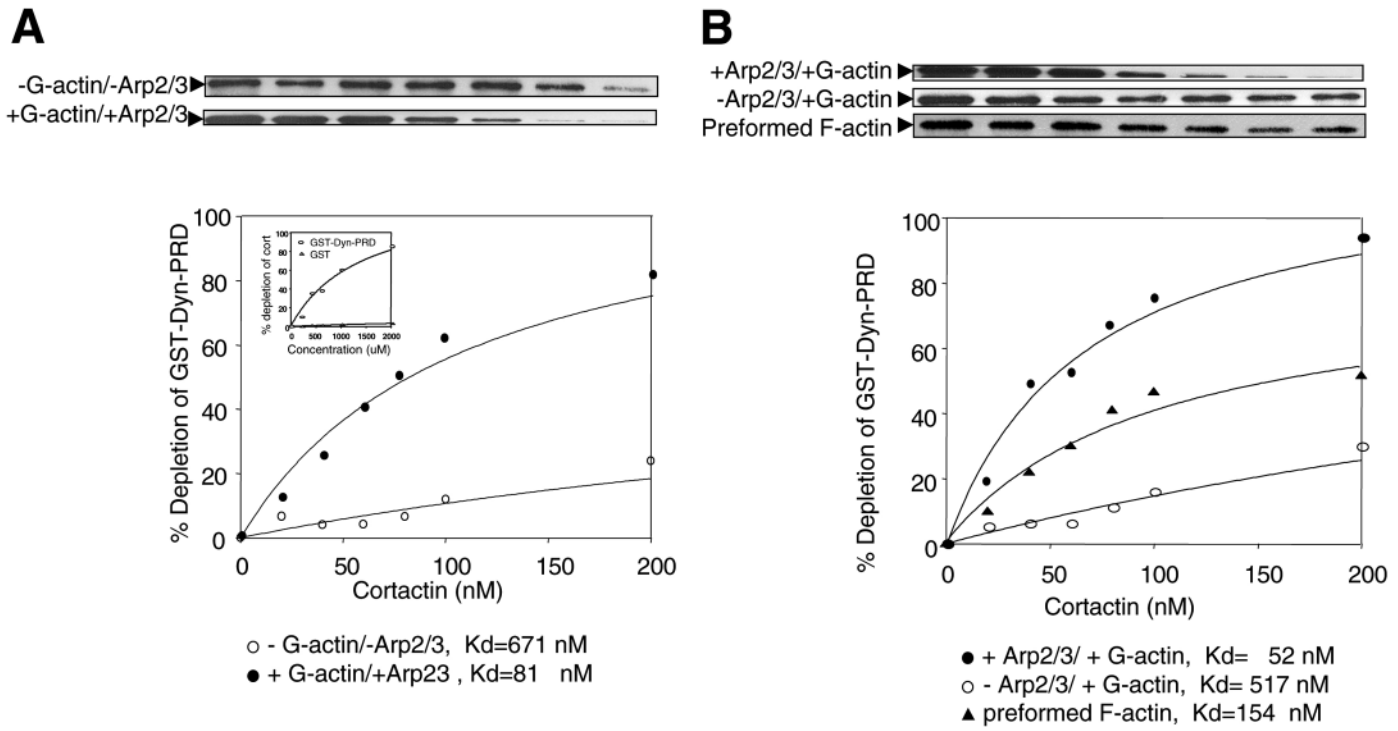

Fig. 6. Actin polymerization regulates the interaction between cortactin and dynamin. (A) Purified GST-Dyn-PRD (30 nM) was mixed with immobilized His-cortactin ranging from 0-200 nM in actin polymerization buffer plus G-actin (2 μM) and Arp2/3 complex (200 nM), and incubated at room temperature for 30 minutes. As a control, the reaction was also performed in the same buffer without G-actin and Arp2/3 complex. The samples were briefly centrifuged and the supernatants were analyzed for the presence of remaining GST-Dyn-PRD by immunoblotting with GST antibody. Amounts of GST-Dyn-PRD on the blot were quantified by digital scanning and normalized to the percentage of depletion. The resulting data were used to fit a rectangular hyperbola, yielding apparent K_d values as indicated. Inset, showing that GST has little binding activity to cortactin as compared to GST-Dyn-PRD. (B) The interaction of GST-Dyn-PRD and cortactin was carried out with G-actin plus Arp2/3 complex or G-actin without Arp2/3 complex. Cortactin was also preincubated with G-actin and Arp2/3 complex for 20 minutes prior to incubation with GST-Dyn-PRD for additional 20 minutes.

Actin polymerization enhances the interaction between cortactin and dynamin 2

To study the role of actin assembly in the regulation of the interaction between cortactin and dynamin 2 in more detail, we examined the interaction between recombinant cortactin and a GST-tagged dynamin PRD peptide (GST-Dyn-PRD). A far-western blot assay confirmed that the interaction between cortactin and GST-Dyn-PRD is direct because GST-Dyn-PRD can probe specifically His-cortactin but not Arp2/3 complex or actin (Fig. 5A). Furthermore, GST-Dyn-PRD, but not GST, can effectively pull-down cortactin in cell lysates (Fig. 5B).

Next, we analyzed the effect of actin polymerization on the affinity of GST-Dyn-PRD for cortactin. Purified GST-Dyn-PRD was mixed with bead-immobilized cortactin tagged with six histidines (His-cortactin) at varying concentrations under conditions with and without Arp2/3 complex and monomeric actin (G-actin). After a 30-minute incubation, GST-Dyn-PRD was pulled down by immobilized His-cortactin and the remaining GST-Dyn-PRD in the supernatant after centrifugation was detected by immunoblot with GST-antibody. As GST-Dyn-PRD did not bind to F-actin (Fig. 5A) and cortactin was not able to pull down GST (Fig. 6A, inset), coprecipitation of GST-Dyn-PRD and cortactin reflected a direct interaction between PRD and cortactin. Using this assay, we estimated that the dissociation equilibrium constant (K_d) of His-cortactin for GST-Dyn-PRD was about 671 nM in the absence of actin polymerization and 81 nM in the presence of Arp2/3 complex and actin (Fig. 6A). To determine whether the increased affinity requires the actin filaments that were assembled specifically by Arp2/3 complex, a binding assay was performed in the presence of G-actin but without the Arp2/3 complex, a condition that was able to yield non-branched actin filaments spontaneously. Under this condition, a K_d of 517 nM was estimated for cortactin to bind to GST-Dyn-PRD (Fig. 6B), which was similar to that in the absence of both actin and the Arp2/3 complex. We were also interested in whether an effective interaction with dynamin requires cortactin that was actively engaged in actin polymerization, which would further support the dynamic interaction between cortactin and dynamin. Therefore, actin was pre-assembled by cortactin and the Arp2/3 complex for 20 minutes prior to adding GST-Dyn-PRD. Under these conditions, the cortactin associated with preformed actin filaments showed a lower affinity for GST-Dyn-PRD with a K_d of 154 nM (Fig. 6B). In contrast, a K_d of 54 nM was estimated in a parallel experiment where the interaction between cortactin and GST-Dyn-PRD took place simultaneously with actin polymerization. These data demonstrated that the cortactin that is actively engaged in Arp2/3-mediated actin polymerization serves as an optimal target for PRD of dynamin 2.

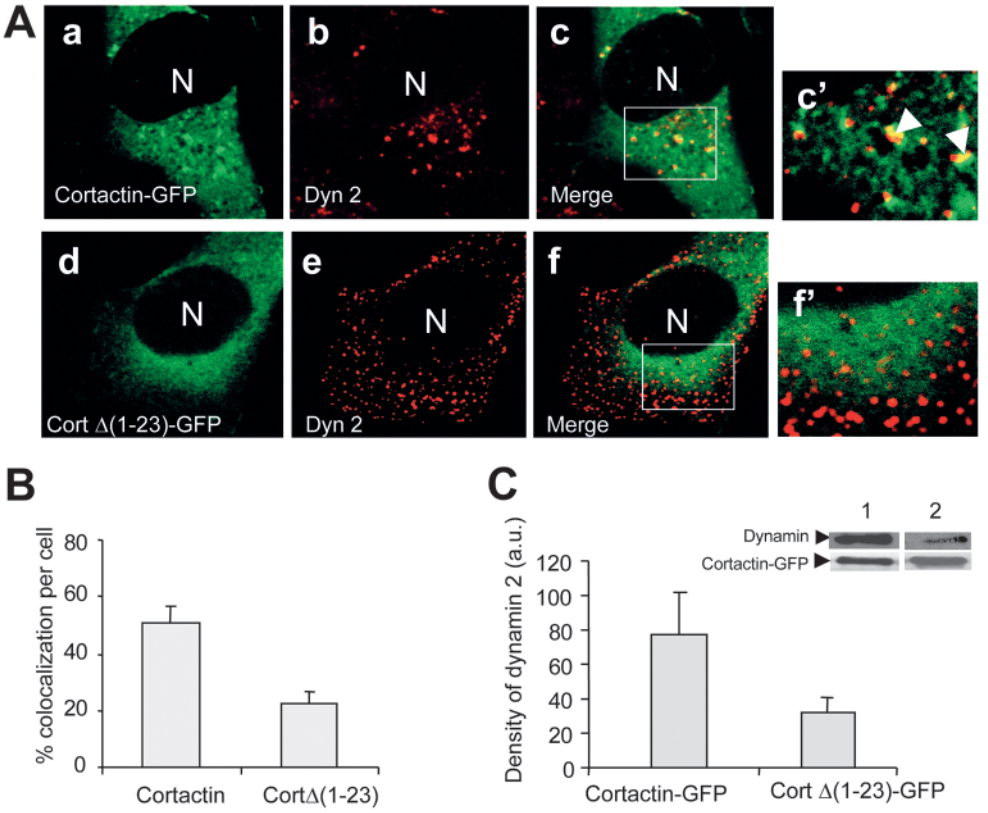

Fig. 7. Binding to Arp2/3 complex is required for cortactin to recruit to dynamin 2. (A) MDA-MB-231 cells expressing cortactin-GFP or CortΔ(1-23)-GFP were grown in 10% serum medium and immunostained with GFP (a and d) or dynamin 2 antibody (b and e) as indicated. The stained cells were examined by confocal microscopy. Magnified images corresponding to the indicated boxes in merged pictures (c and f) are shown in c′ and f′. Two dynamin structures that were closely associated with cortactin-GFP in panel c′ are indicated by arrows. Magnification ×1000. (B) Quantification of colocalization of cortactin-GFP and endogenous dynamin 2 using Optimas 5.2 image-analysis software. The data shown represent the mean±s.d. (*n*=20). (C) Cells expressing cortactin GFP variants were incubated with bio-transferrin for 10 minutes, lysed and subjected to immunoprecipitation with GFP antibody and further analyzed for the presence of cortactin and dynamin 2 by immunoblot assay. A representative blot is shown in the inset. The positions for dynamin 2 and cortactin GFP proteins are indicated. The density of the bands on the blot was digitalized and quantified. The data shown are the mean±s.d. of two independent experiments.

Interaction between cortactin and Arp2/3 complex is required for endocytosis

The above data also suggested that actin polymerization mediated by cortactin and the Arp2/3 complex plays a role in endocytosis. Because cortactin binds directly to the Arp2/3 complex and the binding is necessary for cortactin-mediated actin assembly (Uruno et al., 2001), we reasoned that the interaction with the Arp2/3 complex may be also required for the interaction between cortactin and dynamin 2 in the cell. The domain of cortactin responsible for Arp2/3 binding is within the first 23 amino acids of the N-terminus (Uruno et al., 2001). Mutant CortΔ(1-23)-GFP does not bind to the Arp2/3 complex but is able to inhibit cortactin-mediated actin polymerization in vitro (Li et al., 2004). Interaction between CortΔ(1-23)-GFP and dynamin 2 was examined in MDA-MB-231 breast tumor cells where CortΔ(1-23)-GFP was expressed through a retroviral vector. As a control, colocalization of cortactin-GFP and dynamin 2 was also examined. Dynamin 2 was stained with a polyclonal antibody, and GFP cortactin proteins were visualized directly by fluorescence microscopy. Like endogenous cortactin, cortactin-GFP was localized as cytoplasmic patches, many of which evidently colocalized with dynamin puncta (Fig. 7A a-c). Mutant CortΔ(1-23)-GFP was also distributed in the cytoplasm. However, it did not form patches (Fig. 7A d-f). Furthermore, the degree of colocalization of the mutant with dynamin 2 was reduced to 20%, which was significantly lower than the 44.7% found in cortactin-GFP expressing cells (Fig. 7B). The interaction between cortactin GFP variants with dynamin 2 was further evaluated by immunoprecipitation in the cells. Coprecipitation of dynamin 2 with CortΔ(1-23)-GFP was reduced when compared to cortactin-GFP, confirming that interaction with Arp2/3 complex is necessary for cortactin to interact efficiently with dynamin 2 (Fig. 7C).

Next, we examined transferrin endocytosis in cells expressing cortactin-GFP and CortΔ(1-23)-GFP at different times after cells were treated with transferrin. In addition, we also analyzed the cells expressing CortΔSH3-GFP, which does not bind to dynamin 2. All the GFP fusion proteins were expressed at a very similar level as the endogenous cortactin (Fig. 8A). Although uptake of transferrin was equally efficient in the cells expressing vector or cortactin GFP variants (Fig. 8B), the rate of transferrin internalization was reduced by approximately 41.3% in the cells expressing CortΔ(1-23)-GFP and by 27.6% with CortΔSH3-GFP cells. The degree of the decrease of endocytosis in mutant expressing cells is apparently less than that shown by the cells treated with RNAi (30%). This may suggest that not all cortactin-mediated endocytosis involves Arp2/3 and dynamin interaction. However, CortΔ(1-23)-GFP displayed a quite diffuse distribution in the cytoplasm (Fig. 7Ad) and CortΔSH3-GFP was found in both the cytoplasm and the nucleus (data not shown). Thus, it is more likely that not every mutant molecule in the cell was able to compete with the endogenous cortactin. In summary, this result demonstrated that the interactions of cortactin/Arp2/3 complex and cortactin/dynamin 2 are both required for efficient endocytosis.

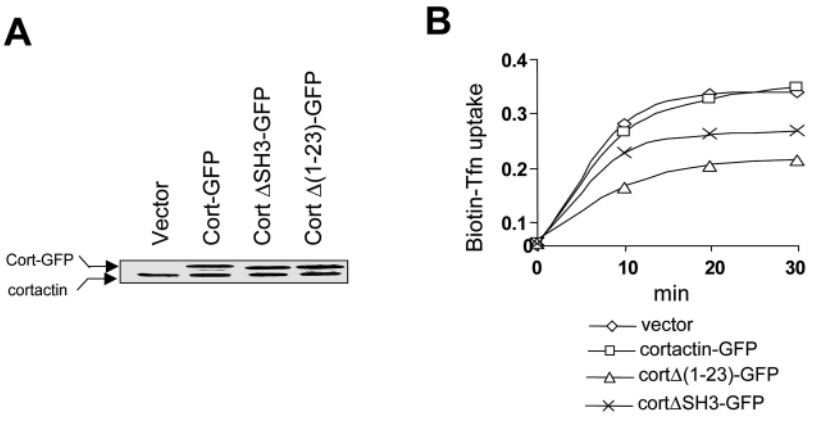

Fig. 8. Arp2/3 complex binding is required for cortactin to interact with dynamin 2. (A) Expression of cortactin fusion proteins was analyzed by immunoblotting whole cell lysates with cortactin antibody. (B) 2×10^5Cells expressing cortactin-GFP fusions were seeded on a 12-well plate, grown in a serum-free medium at 37°C for 30 minutes and incubated with biotin-transferrin for 40 minutes on ice to allow sufficient binding. Endocytosis was initiated by incubation at 37°C for the times as indicated and terminated by placing on ice. The treated cells were then subjected to ELISA-based biotin-transferrin uptake assay as described in Materials and Methods.

Discussion

The role of actin polymerization in efficient uptake of extracellular molecules such as receptor-mediated endocytosis has been well documented. However, the mechanism by which actin polymerization drives endocytosis is unclear. In fact, actin polymerization takes place by adding monomers to the plus end of existing actin filaments, which normally points to the plasma membrane and serves a primary mechanism for membrane protrusion and lamellipodia formation. In contrast, invagination of endocytic vesicles is essentially an inward movement, moving away from the edge of the membrane. Therefore, illustration of a molecular mechanism responsible for such actin polymerization-dependent inward movement is essential to obtain an insight into the initiation of endocytosis and signal transduction. The result presented in this study implies that cortactin is a likely candidate to drive the endocytosis-mediated inward movement in an actin polymerization-dependent manner because it binds to dynamin 2 only in the presence of actin polymerization and associates tightly with a pointed end of growing actin filaments, the combination of which is likely to generate an inward movement.

A recent study has reported that recombinant dynamin induces a modest increase in cortactin-mediated actin polymerization (Schafer et al., 2002). Therefore, the association of dynamin with cortactin may trigger the actin assembly and push the movement of CCVs (Cao et al., 2003). Although a similar mechanism has been used to explain intracellular bacterial movement and membrane protrusion (Pollard and Borisy, 2003), it is hard to understand how such dynamin/cortactin-mediated assembly could lead to invagination of CCVs or inward movement. In fact, our study indicates that actin polymerization mediated directly by dynamin is likely to be minimal because an optimal interaction between dynamin and cortactin appears to be dependent upon actin polymerization itself. This conclusion is based on the following observations. First, actin assembly inhibitor cytochalasin D inhibited colocalization of cortactin and dynamin within cells as well as their direct interaction in cell lysate as shown by immunoprecipitation. Separation of cortactin from dynamin in the presence of cytochalasin D was kinetically correlated with the diminished endocytosis induced by the drug. The second evidence is that the cortactin mutant CortΔ(1-23), which is deficient in Arp2/3 binding and lacks the ability to induce actin assembly (Uruno et al., 2001), colocalized less efficiently with dynamin within cells. The reduced colocalization was not due to the inability to bind to dynamin because the mutant maintains the SH3, the domain that is responsible for dynamin binding. A plausible explanation is that the SH3 domain of the mutant may not be accessible to dynamin. Interestingly, a cortactin mutant containing the

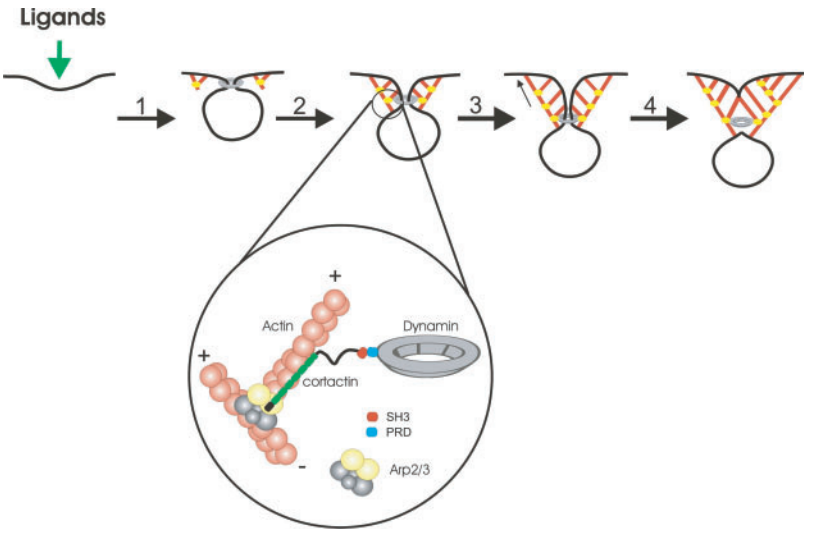

Fig. 9. A model for cortactin- and dynamin-mediated fission of CCV. Step 1, binding of an extracellular ligand to its membrane receptor induces formation of a clathrin-coated pit and recruitment of dynamin to the neck of an invaginated vesicle where it is oligomerized to form a ring structure (for simplicity, only one dynamin ring is shown). The ligand/receptor interaction also triggers assembly of actin (orange line) by activation of WASP family proteins, the Arp2/3 complex and cortactin, resulting ultimately in a tight association of cortactin/Arp2/3 complex at a branched site (yellow circle). Step 2, while the actin polymerization is taking place, the SH3 domain of cortactin at a branching site becomes accessible for interaction with the PRD of dynamin at vesicles. Detail of the interactions between F-actin, cortactin, Arp2/3 complex and dynamin is presented. Step 3, elongation of actin filaments makes the complex of cortactin and dynamin away from the barbed end or its associated plasma membrane and eventually results in the separation of the vesicle from the plasma membrane (Step 4).

cortactin SH3 domain alone is sufficient to translocate into dynamin-associated puncta once it is overexpressed in the cell (data not shown). Therefore, these data strongly indicate that the mutant assumes an autoinhibitory configuration in which the function of the SH3 domain is blocked. The similar autoinhibition probably also exists with wild-type cortactin. However, such autoinhibition may be released upon actin polymerization and endocytosis. In contrast, CortΔ(1-23) mutant, which does not bind to the Arp2/3 complex and consequently is not able to associate effectively at the pointed end of growing actin filaments, becomes constitutively inactive. The final evidence is that the affinity of cortactin for the dynamin PRD domain is increased upon actin polymerization. Although the K_d of Dyn-PRD for cortactin as measured in vitro was about 671 nM, it was dramatically reduced to 81 nM when it was measured under the conditions for actin assembly. It is apparent that the actin-dependent regulation of the SH3 domain requires the function of Arp2/3 because actin filaments assembled by a spontaneous process had no effect on the affinity of cortactin for Dyn-PRD. Furthermore, cortactin that had been pre-associated with branched actin filaments prior to exposure to Dyn-PRD peptides also displayed a reduced affinity compared to that displayed during actin polymerization. However, the presence of the Arp2/3 complex without actin is unable to induce significant increase in the affinity (data not shown). Taken together, both Arp2/3 binding and the cortactin-mediated actin polymerization appear to be necessary to optimize the interaction between cortactin and dynamin.

Our previous studies and others have demonstrated that cortactin promotes both Arp2/3 complex-mediated actin polymerization and branching (Uruno et al., 2001; Weaver et al., 2001). Importantly, cortactin does so by stabilizing an Arp2/3 complex at the pointed end of a daughter actin filament through binding to both the complex and nascent actin filaments (Uruno et al., 2003). As the affinity of cortactin for the Arp2/3 complex during the process of actin assembly is much stronger than that without actin polymerization (25 nM compared to ~1 μM), the complex of cortactin and Arp2/3 at a branching site or the pointed end of a nascent actin filament is tight, resulting in cortactin moving away from the growing barbed end while the actin filament elongates. Based on the data presented here and our previous observations, we propose a model as depicted in Fig. 9 for the events that would best fit the existing data and illustrate a possible mechanism for the vesicle fission mediated by cortactin/dynamin interaction. Briefly, ligand binding to the membrane receptor triggers both recruitment of dynamin into the neck of invaginating vesicles and actin polymerization underneath the plasma membrane in proximity to the site for endocytosis. Actin polymerization is probably facilitated by activation of small GTPases, WASP-like proteins, the Arp2/3 complex and cortactin (Uruno et al., 2003). In the process of actin polymerization, cortactin is further recruited to the Arp2/3 complex at branching sites with nascent actin filaments, resulting in its SH3 domain becoming available for access by dynamin. Although the mechanism for the recruitment of dynamin to CCVs where it is oligomerized to rings and spirals is still not known, the C-terminal PRD domain of the oligomeric dynamin is probably extended from the ring and becomes accessible to the exposed cortactin SH3 domain at actin branching sites (Cao et al., 2003). The enhanced interaction between dynamin and cortactin could further substantiate actin assembly (Schafer et al., 2002). Because the affinity between cortactin and dynamin and that between cortactin and the branching site are significantly enhanced during actin polymerization, it will drive the cortactin-associated dynamin to move along with the actin filaments and take the dynamin away from the growing barbed end, which normally points to the plasma membrane. Such coordinated interactions will generate a force facilitating an eventual fission of the vesicles in concert with the functions of other dynamin partners such as Abp1 and syndapin, which are also known to bind to dynamin through their C-terminal SH3 domains (Kessels et al., 2001; Qualmann and Kelly, 2000). After or at the fission of the vesicles into the cytosol, dynamin is released, which may be either incorporated into cortactin-enriched actin tails as described (Orth et al., 2002), or dissociate from cortactin after cortical actin filaments are dissembled.

Our model agrees with a recent observation that actin assembly starts 100-200 nm from CCVs after recruitment of dynamin to CCVs (Merrifield et al., 2002). It is also consistent with the observations made by others and here that dynamin 2 colocalizes with cortactin only in the area where active actin assembly occurs (Cao et al., 2003; McNiven et al., 2000). It is interesting to note that in addition to dynamin, cortactin also binds to a variety of cellular proteins including ZO-1, CorBP-1, MLCK, Cd2Ap, WIP and CortBP90 (Du et al., 1998; Dudek et al., 2002; Katsube et al., 1998; Kinley et al., 2003; Lynch et al., 2003; Ohoka and Takai, 1998), many of which are also located in proximity to the plasma membrane. Thus, the actin polymerization that regulates the accessibility of cortactin to SH3-binding proteins may provide a general mechanism to drive a dynamic movement associated with membrane organelles participating in endocytosis, phagocytosis, synapse formation and exocytosis.

The authors thank Mark A. McNiven, Hong Cao and Jing Chen at the Mayo Clinic for the dynamin2-GFP plasmids and dynamin polyclonal antibody. This research was supported by NIH grants R01 HL 52753-09, R01 CA-91984-01 to X.Z.

References

Bottomley, M. J., Lo Surdo, P. and Driscoll, P. C. (1999). Endocytosis: how dynamin sets vesicles PHree! *Curr. Biol.* **9**, R301-R304.

Cao, H., Orth, J. D., Chen, J., Weller, S. G., Heuser, J. E. and McNiven, M. A. (2003). Cortactin is a component of clathrin-coated pits and participates in receptor-mediated endocytosis. *Mol. Cell. Biol.* **23**, 2162-2170.

Carter, L. L., Redelmeier, T. E., Woollenweber, L. A. and Schmid, S. L. (1993). Multiple GTP-binding proteins participate in clathrin-coated vesicle-mediated endocytosis. *J. Cell Biol.* **120**, 37-45.

Cousin, M. A. (2000). Synaptic vesicle endocytosis: calcium works overtime in the nerve terminal. *Mol. Neurobiol.* **22**, 115-128.

David, C., McPherson, P. S., Mundigl, O. and de Camilli, P. (1996). A role of amphiphysin in synaptic vesicle endocytosis suggested by its binding to dynamin in nerve terminals. *Proc. Natl. Acad. Sci. USA* **93**, 331-335.

Deitcher, D. (2002). Exocytosis, endocytosis, and development. *Semin. Cell Dev. Biol* **13**, 71-76.

Du, Y., Weed, S. A., Xiong, W. C., Marshall, T. D. and Parsons, J. T. (1998). Identification of a novel cortactin SH3 domain-binding protein and its localization to growth cones of cultured neurons. *Mol. Cell. Biol.* **18**, 5838-5851.

Dudek, S. M., Birukov, K. G., Zhan, X. and Garcia, J. G. (2002). Novel interaction of cortactin with endothelial cell myosin light chain kinase. *Biochem. Biophys. Res. Commun.* **298**, 511-519.

Engqvist-Goldstein, A. E. and Drubin, D. G. (2003). Actin assembly and endocytosis: from yeast to mammals. *Annu. Rev. Cell Dev. Biol.* **19**, 287-332.

Gout, I., Dhand, R., Hiles, I. D., Fry, M. J., Panayotou, G., Das, P., Truong, O., Totty, N. F., Hsuan, J. and Booker, G. W. (1993). The GTPase dynamin binds to and is activated by a subset of SH3 domains. *Cell* **75**, 25-36.

Hill, E., van Der Kaay, J., Downes, C. P. and Smythe, E. (2001). The role of dynamin and its binding partners in coated pit invagination and scission. *J. Cell Biol.* **152**, 309-323.

Hinshaw, J. E. (2000). Dynamin and its role in membrane fission. *Annu. Rev. Cell Dev. Biol* **16**, 483-519.

Hufner, K., Higgs, H. N., Pollard, T. D., Jacobi, C., Aepfelbacher, M. and Linder, S. (2001). The verprolin-like central (vc) region of Wiskott-Aldrich syndrome protein induces Arp2/3 complex-dependent actin nucleation. *J. Biol. Chem.* **276**, 35761-35767.

Kaksonen, M., Peng, H. B. and Rauvala, H. (2000). Association of cortactin with dynamic actin in lamellipodia and on endosomal vesicles. *J. Cell Sci.* **113**, 4421-4426.

Katsube, T., Takahisa, M., Ueda, R., Hashimoto, N., Kobayashi, M. and Togashi, S. (1998). Cortactin associates with the cell-cell junction protein ZO-1 in both Drosophila and mouse. *J. Biol. Chem.* **273**, 29672-29677.

Kessels, M. M., Engqvist-Goldstein, A. E., Drubin, D. G. and Qualmann, B. (2001). Mammalian Abp1, a signal-responsive F-actin-binding protein, links the actin cytoskeleton to endocytosis via the GTPase dynamin. *J. Cell Biol.* **153**, 351-366.

Kinley, A. W., Weed, S. A., Weaver, A. M., Karginov, A. V., Bissonette, E., Cooper, J. A. and Parsons, J. T. (2003). Cortactin interacts with WIP in regulating Arp2/3 activation and membrane protrusion. *Curr. Biol.* **13**, 384-393.

Li, Y., Tondravi, M., Liu, J., Smith, E., Haudenschild, C. C., Kaczmarek, M. and Zhan, X. (2001). Cortactin potentiates bone metastasis of breast cancer cells. *Cancer Res.* **61**, 6906-6911.

Li, Y., Uruno, T., Haudenschild, C. C., Dudek, S. M., Garcia, J. G. and Zhan, X. (2004). Interaction of cortactin and Arp2/3 complex is required for sphingosine-1-phosphate induced endothelial cell remodeling. *Exp. Cell Res.* **298**, 107-121.

Liu, J., Huang, C. and Zhan, X. (1999). Src is required for cell migration and shape changes induced by fibroblast growth factor 1. *Oncogene* **18**, 6700-6706.

Lynch, D. K., Winata, S. C., Lyons, R. J., Hughes, W. E., Lehrbach, G. M., Wasinger, V., Corthals, G., Cordwell, S. and Daly, R. J. (2003). A Cortactin-CD2-associated protein (CD2AP) complex provides a novel link between epidermal growth factor receptor endocytosis and the actin cytoskeleton. *J. Biol. Chem.* **278**, 21805-21813.

McNiven, M. A., Kim, L., Krueger, E. W., Orth, J. D., Cao, H. and Wong, T. W. (2000). Regulated interactions between dynamin and the actin-binding protein cortactin modulate cell shape. *J. Cell Biol.* **151**, 187-198.

Merrifield, C. J., Feldman, M. E., Wan, L. and Almers, W. (2002). Imaging actin and dynamin recruitment during invagination of single clathrin-coated pits. *Nat. Cell Biol.* **4**, 691-698.

Ohoka, Y. and Takai, Y. (1998). Isolation and characterization of cortactin isoforms and a novel cortactin-binding protein, CBP90. *Genes Cells* **3**, 603-612.

Orth, J. D. and McNiven, M. A. (2003). Dynamin at the actin-membrane interface. *Curr. Opin. Cell Biol.* **15**, 31-39.

Orth, J. D., Krueger, E. W., Cao, H. and McNiven, M. A. (2002). The large GTPase dynamin regulates actin comet formation and movement in living cells. *Proc. Natl. Acad. Sci. USA* **99**, 167-172.

Pollard, T. D. and Borisy, G. G. (2003). Cellular motility driven by assembly and disassembly of actin filaments 22. *Cell* **112**, 453-465.

Qualmann, B. and Kelly, R. B. (2000). Syndapin isoforms participate in receptor-mediated endocytosis and actin organization. *J. Cell Biol.* **148**, 1047-1062.

Qualmann, B. and Kessels, M. M. (2002). Endocytosis and the cytoskeleton. *Int. Rev. Cytol.* **220**, 93-144.

Qualmann, B., Roos, J., DiGregorio, P. J. and Kelly, R. B. (1999). Syndapin I, a synaptic dynamin-binding protein that associates with the neural Wiskott-Aldrich syndrome protein. *Mol. Biol. Cell* **10**, 501-513.

Ramjaun, A. R., Micheva, K. D., Bouchelet, I. and McPherson, P. S. (1997). Identification and characterization of a nerve terminal-enriched amphiphysin isoform. *J. Biol. Chem.* **272**, 16700-16706.

Ringstad, N., Nemoto, Y. and de Camilli, P. (1997). The SH3p4/Sh3p8/SH3p13 protein family: binding partners for synaptojanin and dynamin via a Grb2-like Src homology 3 domain. *Proc. Natl. Acad. Sci. USA* **94**, 8569-8574.

Roos, J. and Kelly, R. B. (1998). Dap160, a neural-specific Eps15 homology and multiple SH3 domain-containing protein that interacts with Drosophila dynamin. *J. Biol. Chem.* **273**, 19108-19119.

Schafer, D. A., Weed, S. A., Binns, D., Karginov, A. V., Parsons, J. T. and Cooper, J. A. (2002). Dynamin2 and cortactin regulate actin assembly and filament organization. *Curr. Biol.* **12**, 1852-1857.

Schmid, S. L. and Smythe, E. (1991). Stage-specific assays for coated pit formation and coated vesicle budding in vitro. *J. Cell Biol.* **114**, 869-880.

Sever, S. (2002). Dynamin and endocytosis. *Curr. Opin. Cell Biol.* **14**, 463-467.

Simpson, F., Hussain, N. K., Qualmann, B., Kelly, R. B., Kay, B. K., McPherson, P. S. and Schmid, S. L. (1999). SH3-domain-containing proteins function at distinct steps in clathrin-coated vesicle formation. *Nat. Cell Biol.* **1**, 119-124.

Smythe, E., Carter, L. L. and Schmid, S. L. (1992). Cytosol- and clathrin-dependent stimulation of endocytosis in vitro by purified adaptors. *J. Cell Biol.* **119**, 1163-1171.

Uruno, T., Liu, J., Zhang, P., Fan, Y., Egile, C., Li, R., Mueller, S. C. and Zhan, X. (2001). Activation of Arp2/3 complex-mediated actin polymerization by cortactin. *Nat. Cell Biol.* **3**, 259-266.

Uruno, T., Liu, J., Li, Y., Smith, N. and Zhan, X. (2003). Sequential interaction of actin-related proteins 2 and 3 (Arp2/3) complex with neural Wiscott-Aldrich syndrome protein (N-WASP) and cortactin during branched actin filament network formation. *J. Biol. Chem.* **278**, 26086-26093.

Weaver, A. M., Karginov, A. V., Kinley, A. W., Weed, S. A., Li, Y., Parsons, J. T. and Cooper, J. A. (2001). Cortactin promotes and stabilizes Arp2/3-induced actin filament network formation. *Curr. Biol.* **11**, 370-374.

Witke, W., Podtelejnikov, A. V., di Nardo, A., Sutherland, J. D., Gurniak, C. B., Dotti, C. and Mann, M. (1998). In mouse brain profilin I and profilin II associate with regulators of the endocytic pathway and actin assembly. *EMBO J.* **17**, 967-976.

Journal of Cell Science